ГОДИШНИК НА УНИВЕРСИТЕТА ПО АРХИТЕКТУРА, СТРОИТЕЛСТВО И ГЕОДЕЗИЯ
СОФИЯ

Том Volume 57 2024 Брой Issue 1

ANNUAL OF THE UNIVERSITY OF ARCHITECTURE, CIVIL ENGINEERING AND GEODESY
SOFIA

DOI: 10.71167/uaceg.2024.570109

Получена: 17.05.2023 г.
Приета: 18.06.2023 г.

ENERGY-EQUIVALENT APPROACH FOR SOLVING NONLINEAR EQUATIONS BY FEM USING GENERALIZED HYPERBOLIC STRESS-STRAIN RELATIONSHIP

A. Alexandrov[1]

Keywords: *material nonlinearity, stress-strain relationship, hyperbolic functions, small deformations, strain energy, nonlinear finite element analysis, incremental-iterative solution*

ABSTRACT

A simple, robust, and powerful original computational approach to solve the quasi-static problem is presented in which the behavior of solids with material nonlinearity is modeled by the behavior of energy-equivalent with respect to the strain energy pseudo-perfect elastic solid. This method does not fail for stress-strain curves having inflection points or other peculiarities, and the mathematical convergence of the solution breaks only when the solids become physically destroyed. It is shown cogently that an appropriate classical iterative procedure can be simpler, more efficient and several times faster compared to the regular, the modified Newton-Raphson method, or other often used numerical methods, and the use of the displacements in perfect elastic solid as the initial value for solving the nonlinear equations has significant advantages and is a better first iteration prediction for the displacements than the usually used prediction $\{d^0\}=\{0\}$.

1. Introduction

Realistic modeling and correct prediction of the natural physically nonlinear behavior of various types of materials is an extremely important part of both theoretical and applied or computational mechanics. This branch of physics has been developed for more than a century and has gained great momentum in recent decades. The classical model of Linear Elasticity does not give a correct picture of the real mechanical behavior of the solids, as it does not

[1] Alexander Alexandrov, M.Sc., ENERGOEXPERT AD, 20 Kosta Lulchev St., Sofia 1113,
e-mail: alexander.alexandrov.63@gmail.com

consider the different degrees of failures, nor can it truthfully describe the limiting values of the forces that a structure can sustain before it loses its load-bearing capacity according to one criterion or another. In order to find answers to these questions, dozens of material nonlinearity models have been developed, e.g. [1 – 5], and many mathematical methods have been applied to solve the system of nonlinear equations, e.g. [6 – 13]. A number of computer programs have been developed DIANA FEA, PLAXIS, ABACUS, ANSYS, NASTRAN, Dlubal Software, ADINA, SAP 2000, NISA etc. In addition to the huge variety of physical models of material behavior, which are not very easy to use in practice, the basic challenge is to ensure the convergence of the problem. In not a few cases used standard or modified Newton-Raphson scheme and most quasi-static methods fail. Furthermore, some of the successfully applied methods, especially in larger-scale problems, involve big computational efforts and considerable computational time, e.g. [14], etc.

To overcome these difficulties, the aim is to approximate the nonlinear behavior of different types of materials as quasi-linear, where, and as far as possible. This would greatly simplify both the formulation and the solution of the system of equations. On the other hand, the simple but natural modelling of different types of material nonlinearity and the solution of the nonlinear problem by the standard Finite element method, based entirely on the behavior of a linear-elastic material, would greatly extend the practical application of the Nonlinear Mechanics. Her use not infrequently meets insufficient understanding by structural engineering students [15] and structural engineers due to excessive complexity of theoretical models and not small difficulties to obtain easy applicable in practice result. This paper presents some simple iterative approaches in the standard Finite element method to find a fast convergent and stable solution of the system of nonlinear equations in the case where the body is not fully destroyed in any region due to the applied load. Then the failure process can be traced to the collapse and its onset predicted. The proposed methods for solving the nonlinear equations by FEM in the case of material nonlinearity in solids can be applied to any physical model. In this study, a material nonlinearity model using hyperbolic functions was chosen because of its simple, compact, and well-conditioned form from a physical point of view. With this model, a wide variety of stress-strain relationships can be easily defined, both for plastic and brittle or hyperelastic materials. This model describes the material nonlinearity in various types of solids with simple analytical functions and only a few natural scalar parameters for the stresses and strains.

2. Energy-equivalent approach for the solving of the equations of the material nonlinearity in quasi-static finite element analysis

In the classical mathematical approach to solving systems of linear or nonlinear equations, we are usually not interested in exactly how these equations are derived and not infrequently underestimate their physical meaning when searching for a solution. The equilibrium equations of the forces of solid mechanics are a consequence of the Law of Conservation of Energy when all internal and external forces are expressed with respect to the same corresponding "generalized" displacements. This is essentially Castigliano's first theorem, which holds both for a linearly elastic solid and in the case of a nonlinear relationship between the generalized displacements (in this case strains) and the generalized forces (in this case stresses) [16, 17]. Castigliano's first theorem holds whenever the strain energy is obtained after integration of the generalized forces (stresses) with respect to the generalized displacements (strains). In the most general case of material nonlinearity, however, the strain energy cannot be so easily expressed as a function of generalized forces, since the $\sigma(\varepsilon)$

dependency rather than $\varepsilon(\sigma)$ is usually defined, and Castigliano's second theorem does not hold. This problem is overcome by introducing the concept of "specific additional energy", which makes it possible to apply Castigliano's second theorem to a non-linear-elastic body. Essentially, the physical nature of the process is that when displacements due to external forces cause strains in the solid, these in turn cause stresses, not the vice versa. However, since we solve the material nonlinearity problem by modeling the solid as pseudo linear elastic body, we can consider that $\delta\Pi = 0$ and the resulting displacements satisfy the principle of minimum strain energy (Castigliano's Second Theorem – "The Theorem of Least Work" [18]) as well as the condition of uniqueness (Kirchhoff's uniqueness theorem [1, 16]) within the solution. A look back into the physics can help a lot for the mathematical solution. If we turn to the origin of the equations of equilibrium of forces, we can obtain a good solution for the quasi-static problem at material nonlinearity in solid mechanics. The physical nature of the equilibrium conditions is fundamental not only for forming the mechanical model in the case of small deformations, but also it is essential to obtain a robust and fast mathematical solution.

In solving both the linear and nonlinear static problem as a rule it is assumed that the applying of the load is time independent, but in fact it is progressive. The mode of application is the key: it is assumed that the load increases linearly from 0 to its maximum value, i.e., it is applied very slowly, with a constant speed and zero accelerations, so that it does not to induce inertial forces in the solid. This in turn determines a linear increase in external forces, which leads to a corresponding linear increase in displacements in the perfect elastic solid, which has modulus of elasticity that is invariant under load. Clapeyron's theorem [16] defines this process by specifying that the work of external forces is equal to half the work if they act at their maximum value throughout the whole time of loading, or that the strain (internal) energy of an elastically deformed body is equal to half the work. This can be seen in determining of the strain energy potential of solids in case of perfect elasticity: $\sigma = E.\varepsilon$ in expression (1). When the load is applied with its maximum value from the beginning to the end, it produces a dynamic effect which can be defined as "Impact of a body on a weightless structure" [18]. The static load in fact is a real linear time function and does a strictly defined work in each case, depending on the "deformability" of the structure, regardless of whether the material is linear elastic or some type of nonlinear. The nonlinear behavior of the material does not change the linear applied model of the external forces, as this would disturb the static nature of the problem. To avoid this discrepancy some authors, use the definition "pseudo" time when defining the forces increment interval Δt in the Newton-Raphson Method for solving the nonlinear static problem, since time is anyway a parameter of the load. The problem is quasi-static and beside this the load is assumed to be deformation independent as in general all this refers to the maximum (the ultimate) values of the applied forces. The work of external forces and therefore the strain energy depend on the "deformability" and "plasticity" of the structures in every particular case.

For convenience, no limiting the generalizability of the method, the main idea of the proposed approach for solving the nonlinear equations in FEM, obtained for solids with material nonlinearity, will be presented using the following simple stress-strain relationship (see Fig. 1):

$$\sigma(\varepsilon) = \sigma_{lim}.\tanh\left(\frac{\varepsilon}{\varepsilon_{rul}}\right). \tag{1}$$

Formula (1) $\sigma(\varepsilon)$ shows the stress in the elementary volume, defined by the Cauchy stress tensor, and σ_{lim} is its limiting value, which it tends to but does not reach; "ε" is the strain according to Infinitesimal strain theory, defined by the Cauchy's strain tensor, and ε_{rul} is the governing strain, which may be considered and as a limiting value at which failure occurs. Since for any material no strictly defined values can be fixed for the stresses and/or strains at which its failure begins or ends, and these are always a matter of assumption and some chosen criteria, therefore σ_{lim} and ε_{rul} are close to different real limiting values of stresses and strains but they are not exactly some of them. The parameter ε_{rul} can be taken as limiting strain in the cases when its numerical values satisfy the corresponding conditions for the magnitude of the real limiting strain when the body is fully destroyed. From a practical point of view, to get a "good" stress-strain curve, another value for ε_{rul} can be defined, independent of the limiting strain, less or greater than it. Analogical consideration can be used for choosing the limit stress, too. For each stress-strain relationship σ_{lim} – the limit stress value and ε_{rul} – the governing strain are constant parameters.

In the case when the stress is defined by formula (1), the strain will be given by the expression:

$$\varepsilon = \varepsilon_{rul}.\,\text{artanh}\left[\frac{\sigma(\varepsilon)}{\sigma_{lim}}\right] = \frac{1}{2}\varepsilon_{rul}.\ln\left[\frac{\sigma_{lim} + \sigma(\varepsilon)}{\sigma_{lim} - \sigma(\varepsilon)}\right]. \qquad (2)$$

To determine the work of internal forces, we integrate the stress function with respect to the strains, from $\varepsilon = 0$ to $\varepsilon = \varepsilon_{end}$, over a given volume (elementary or finite); ε_{end} is the final strain value up to which the integration of the work of the internal forces – the strain energy – takes place; e.g., in Fig. 2 and formula (3) $\varepsilon_{end} = \varepsilon_t$. This holds both to the linear elastic and material nonlinearity problem in solids. It does not matter if σ–ε relationship is curvilinear or linear: in both cases the strain energy is the area of the diagram between the abscissa "ε" and the corresponding curved or straight line $\sigma = f(\varepsilon)$ for a given value of strain (Fig. 2). Per unit volume we compute the strain energy density by well-known way:

$$W = \int_0^{\varepsilon_t} \sigma(\varepsilon)\mathrm{d}\varepsilon. \qquad (3)$$

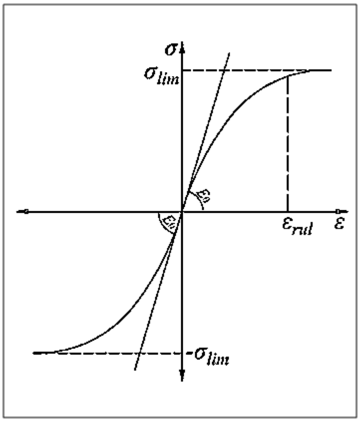

Figure 1. Stress-strain relationship

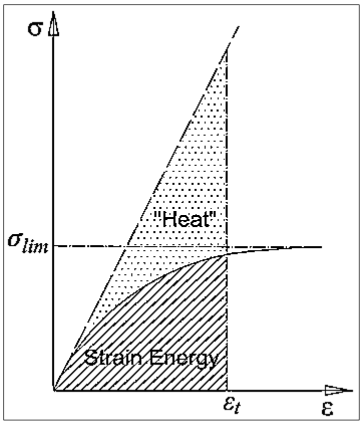

Figure 2. Energy distribution in material nonlinearity

For solving the very complex problem of the material nonlinearity, one seeks a solution approximating it to a quasi-linear elastic problem. Then the very well-developed standard Finite element method can be used. One seeks such a solution when using formula (1) as stress-strain relationship. The procedure to forming the "nonlinear", usually called tangent stiffness matrix according to the FE theory, is to express the work of non-inertial internal forces using the variable modules $E(\varepsilon)_{ij} = \frac{\partial\sigma(\varepsilon)_{ij}}{\partial\varepsilon_{ij}}$. Then for the strain energy in case of nonlinear deformation we get:

$$W_{pl,1} = \int_0^{\varepsilon_t} \Sigma\sigma(\varepsilon)_{ij} \mathrm{d}\varepsilon = \int_0^{\varepsilon_t} \left[\Sigma E(\varepsilon)_{ij}.\varepsilon\right] \mathrm{d}\varepsilon = \int_0^{\varepsilon_t} \left[\Sigma \frac{E_{0,ij}}{\cosh^2\left(\frac{\varepsilon}{\varepsilon_{rul,ij}}\right)}.\varepsilon\right] \mathrm{d}\varepsilon. \quad (4)$$

Using formula (1), the strain energy can be expressed by directly integrating the stress-strain relationship:

$$W_{pl,2} = \int_0^{\varepsilon_t} \Sigma\sigma(\varepsilon)_{ij} \mathrm{d}\varepsilon = \int_0^{\varepsilon_t} \left[\Sigma\sigma_{lim,ij}.\tanh\left(\frac{\varepsilon_t}{\varepsilon_{rul,ij}}\right)\right] \mathrm{d}\varepsilon. \quad (5)$$

For generalization, in expressions (4) and (5) the indices "*ij*" for initial (linear) modules, limiting stresses, and governing strains show the case of different material nonlinearity for each one of Cauchy stress tensor component separately.

The integration of expressions (4) and (5) for an arbitrary (elementary) volume or finite element from $\varepsilon = 0$ to $\varepsilon = \varepsilon_t$ leads to the following result:

$$W_{pl,1} = \sigma_{lim,ij}.\varepsilon_t.\tanh\left(\frac{\varepsilon_t}{\varepsilon_{rul,ij}}\right) - \sigma_{lim,ij}.\varepsilon_{rul,ij}.\ln\left[\cosh\left(\frac{\varepsilon_t}{\varepsilon_{rul,ij}}\right)\right]. \quad (6)$$

$$W_{pl,2} = \sigma_{lim,ij}.\varepsilon_{rul,ij}.\ln\left[\cosh\left(\frac{\varepsilon_t}{\varepsilon_{rul,ij}}\right)\right]. \quad (7)$$

The comparison of the numerical results for $W_{pl,1}$ and $W_{pl,2}$ shows that the correctly computed value for the strain energy of a solid with material nonlinearity by formula (7) is bigger than the approximately computed by formula (6), when using the formulae $\sigma(\varepsilon) = E(\varepsilon).\varepsilon$. This difference increases rapidly with the increase of the integration interval $0 \div \varepsilon_t$. The difference in the strain energy for the case defined by formula (1) when σ_{lim} = 550,0 MPa and ε_{rul} = 0,002619 are shown in Fig. 3. On the other hand, the tangent stiffness matrix $[K(\varepsilon)]$ composed after approximation (4), is not always well-conditioned. In some cases, e.g., when the curve σ–ε has peculiarities as snap through or snap back, this raises several computational difficulties related both to the formation of the tangent stiffness matrix $[K'(\varepsilon)]$, and to the convergence of the problem when applying the Newton-Raphson Method, some modification thereof and even some methods, that do not necessarily use tangent stiffness matrix, like "Line search".

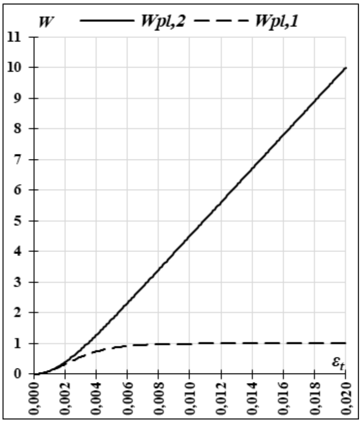

Figure 3. The difference in the strain energy calculated for equations (6) and (7)

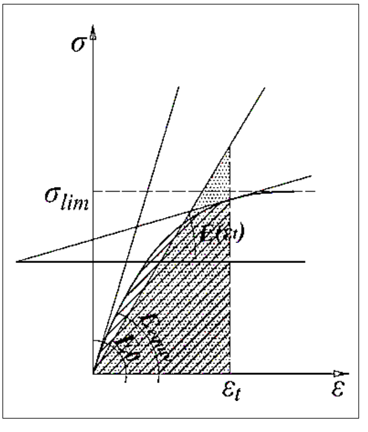

Figure 4. The modules for the Tangent and the Equivalent stiffness matrix

For the use of the standard FEM, it is mandatory to form a "nonlinear" stiffness matrix. Although expression (7) gives the exact value of the strain energy, unlike expression (5), it is not suitable for this purpose. Energy "equivalent" stiffness matrix of a pseudo-linear elastic solid can be composed, so that it gives exactly the work of the (non-inertial) internal forces (strain energy potential) of a material nonlinear solid with stress-strain relationship defined by formula (1) or by some other *σ–ε* relationship:

$$W_{pl,2} = \int_0^{\varepsilon_t} \left[\Sigma \sigma_{lim,ij} . \tanh\left(\frac{\varepsilon}{\varepsilon_{rul,ij}}\right)\right] \mathrm{d}\varepsilon = W_{el,equiv} = \int_0^{\varepsilon_t} (\Sigma E_{equiv,ij} \varepsilon_{ij}) \mathrm{d}\varepsilon. \qquad (8)$$

In equation (8) $E_{equiv,ij}$ is the energy-equivalent linear modulus of elasticity (Young's modulus) of the elementary volume that in fact is some kind of secant modulus of the *σ–ε* curve, not tangent or mean modulus, which are often used.

From expression (8) follows that in order the work of the internal forces of a solid (elementary volume or finite element) with material nonlinearity to be equal to the work of the internal forces of a pseudo-linear elastic solid (for the same volume), the latter must have energy-equivalent linear modulus of elasticity (Young's modulus) obtained from the following expression:

$$W_{pl,2} = W_{el,equiv} = \sigma_{lim,ij} . \varepsilon_{rul,ij} . \ln\left[\cosh\left(\frac{\varepsilon_t}{\varepsilon_{rul,ij}}\right)\right] = \frac{1}{2} E_{equiv,ij} \varepsilon_{ij}^2. \qquad (9)$$

From expressions (7) and (9) follows that in order to compose the "nonlinear" stiffness matrix in the standard FEM, the following energy-equivalent linear modulus of elasticity (Young's modulus) should be used for each finite element (see Fig. 4):

$$E_{equiv,ij} = \frac{\left\{2 . \sigma_{lim,ij} . \varepsilon_{rul,ij} . \ln\left[\cosh\left(\frac{\varepsilon_t}{\varepsilon_{rul,ij}}\right)\right]\right\}}{\varepsilon_{ij}^2}. \qquad (10)$$

The indices "ij" show again that such equivalent linear modulus of elasticity is defined separately for each component of the Cauchy stress tensor.

The energy-equivalent modules of a pseudo-linear elastic solids (or finite elements) can be computed by formula (10) to compose the stiffness matrixes in the standard FEM for each finite element and Cauchy's strain tensor component ε_{ij}, using corresponding $E_{equiv,ij}$. Essentially the resultant global stiffness matrix can be considered as an approximation using the method of the secant and this matrix is fully analogous to the tangent stiffness matrix in regular Newton-Raphson method. The successive composing of the energy-equivalent "nonlinear" stiffness matrixes in each step of the solving of the nonlinear equations (11) using simple incremental-iterative procedure leads to successive approach to the roots:

$$\left[K\left(E_{equiv,ij}\left(\varepsilon_{ij}^k\right)\right)\right] . \{u^{k+1}\} = \{F\}, k = 1, 2, \dots, n. \qquad (11)$$

At each step the maximum values of the external forces $\{F\}$ are applied. As a first prediction the displacements in the structure considered as perfect elastic solid are used, also caused by the maximum values of the load, i.e. for $k = 1$ the strains $\varepsilon_{ij}^{k=1} = 0$ and $\{u^{k=2}\} = \{u_{purf.el.}\}$. Following this procedure at every iteration new energy-equivalent modules are calculated and new "secant" stiffness matrixes $\left[K\left(E_{equiv,ij}\left(\varepsilon_{ij}^k\right)\right)\right]$ for each finite element are composed. $\{F\}$ computes the displacements $\{u^{k+1}\} = \left[K\left(E_{equiv,ij}\left(\varepsilon_{ij}^k\right)\right)\right]^{-1}$ until $\{u^{k+1}\} - \{u^k\} \leq \epsilon$, as "$\epsilon$" is an appropriate convergence criteria. It can be with respect to stresses, strains or displacements.

At first sight it seems laborious solution, but only for few iterations one can obtain a very good-looking result for strains and stresses, respectively for displacements $\{u\}$. Instead of solving nonlinear equations (11) step by step for a small change of the static load, this can be done directly for the final (maximum) value of the external forces. The iterations in this case are only with respect to the variable energy-equivalent modules of the pseudo-linear elastic solid (for each finite element). Starting with initial value of modulus of elasticity and the final (maximum) values of the load, the nonlinearity modules vary according to formula (10) depending only on the calculated displacements and deformations in each iteration. The values of $E_{equiv,ij}$ obtained for each step are put in the next one, until the convergence criteria is satisfied. Essentially, each successive iteration can be considered as a small "time step" Δt where the external load increases incrementally but not by a constant fixed value.

If the solid is not destroyed completely in some region at the specified external forces, the process is stable and rapidly convergent. It breaks down only if sufficient strain energy potential cannot be accumulated in the solid, considering material nonlinearity, so that to be equal to the work of external forces. Each iteration then yields to the gradual destruction of the solid, modifying its physical characteristics, before final collapse occurs. In this case, the displacements continue to increase at each iteration instead of converging to the solution of the problem, since there is no such. In the solution by Finite element method this means the energy-equivalent modules of elasticity for all finite elements at some node will become zero or a very small computational value. Each iteration can also be considered as a step of loading increment. The external forces increase not with equal steps, but with values as a result of the displacements in the corresponding iteration, obtained according to the σ–ε relationship in the problem.

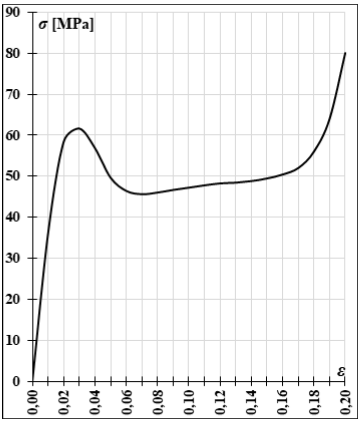

Figure 5. σ–ε curve with inflexion and concavity

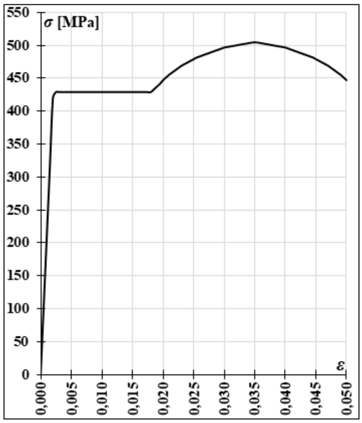

Figure 6. σ–ε curve with convexity

The above described methodology allows to use much more complex σ–ε relationships, than the defined by formula (1). This is very useful from practical point of view. Since the solution used in FEM computation is based on a calculation of the area of the diagram of the σ–ε curve (i.e., real strain energy in solid), the solution of this nonlinear problem can be seriously generalized. Various theoretical types of σ–ε dependences for defining material nonlinearity in solids (and soils) can be used easily, as well as complex true stress-true strain curves. Moreover, the proposed methodology can be used without problems for dependences in which there are inflexion points, convex or concave parts of the σ–ε curves (Fig. 5, Fig. 6, and Fig. 18), which raise serious computational problems in the general case. It should be noted that the σ–ε relationships e.g., on Fig. 5, as well as any other stress-strain function (relationship) that has a negative first derivative ("strain modulus") in some sections, refers to the case where the external load depends on the realized strains. It is presented here for illustrative purposes only to show that in a purely theoretical sense the proposed methodology can also be used for σ–ε curves with similar features.

3. Numerical results and discussion

3.1. Advantages of the Energy-equivalent approach and two simplified iterative procedures in comparison to the regular Newton-Raphson method in solving the nonlinear equation of the quasi-static problem for structural elements with material nonlinearity

The presented methodology for the Energy-equivalent approach for solving the system nonlinear equations in material nonlinearity in the case of small displacements is illustrated by five examples. As a very useful addition to the proposed methodology for solving the nonlinear system of equations in the quasi-static problem, another first prediction for the displacements $\{u\}$ is proposed. Since in all types of nonlinear σ–ε relationships and in all loading cases in material nonlinearity problems in solids the nonlinear displacements always are (it can be said "by definition") larger than the displacements in the same solid considered as linear elastic, it is much more appropriate to use $\{u\} = \{u_{perf.el}\}$ for the first approximation than $\{u\} = \{0\}$; $\{u_{perf.el}\}$ are the displacements due to static load in the linear elastic state of the structure.

This approximation has several important advantages:

– This prediction for the first approximation saves the calculations for the displacements $\{u\}$ until $\{u_{perf.el}\}$ is reached.

– If the values of the internal forces – the reactions of the structure $\{R_{int}\}$ in FEM – as perfect elastic solid are greater than the maximum possible reactions according to the prescribed σ–ε relationship for nonlinear material behavior, then there is no convergence of the solution, and the problem has no solution. The iterations will continue to infinity without satisfying the equilibrium condition $[K(u)].\{u\} = \{F_{ext}\}$, so that the variable stiffness matrix $[K(u)]$ tends steadily to some finite value obtained with the corresponding values of the modules of plastic deformations at which the displacements stop increasing. Physically, this means that the construction cannot withstand the given load and is destroyed in some parts because there is no sufficient load-bearing capacity. When the stiffness matrices of all finite elements connected at some nodes become equal to 0, the solution fails – the global stiffness matrix gets 0 on the main diagonal. To continue solving the problem, it is necessary to set some minimum value for the nonlinear modules of the finite elements, e.g., 1,0 MPa, or recompose the global stiffness matrix by defining the node with $K(u)_{ii} = 0$ two or more times with the same geometric coordinates. In this way, the occurrence of a crack in the structure at that point along the corresponding direction is simulated. The finite elements in this node where 0 has occurred should be "distributed" appropriately among the new nodes at this point to obtain a good simulation of the resulting crack. Cracking as a material nonlinearity is not a subject of this paper.

– A simple incremental-iterative procedure can be utilized to find the root of the equation $[K(u)].\{u\} - \{F_{ext}\} = \{0\}$, working with one and the same proportional step for the displacements $\{u\}$ at each node in relation to the displacement in the perfect elastic solid, until function $f(u) = [K(u)].\{u\} - \{F_{ext}\} = \{0\}$ changes its sign. After that the final solution can be even more precisely determined by a simple triple rule between the last two iterations.

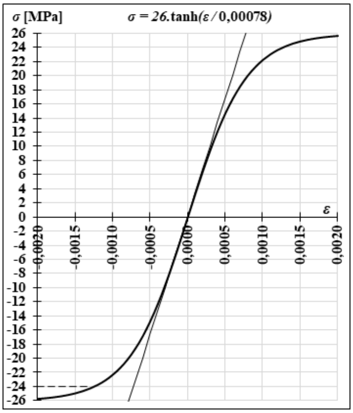

Figure 7. *σ–ε* curve for C30/37 concrete bar column in example in 3.3.1

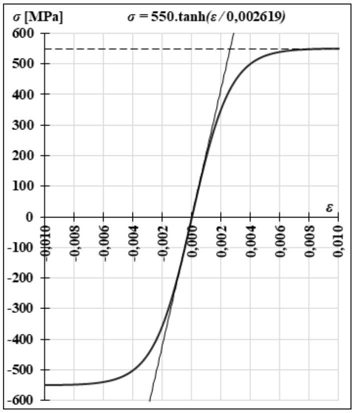

Figure 8. *σ–ε* curve for steel B500B in example in 3.3.2

The above approach is illustrated by two examples given in Sections 3.1.1 and 3.1.2. A C30/37 concrete column loaded to compression and a B500B steel bar loaded to tension are considered. The *σ–ε* relationships are shown in Fig. 7 and Fig. 8, respectively. For both examples the static scheme is a bar with fixed support $u_1 = 0$ and free loaded point with displacement $u_2 = u$. Since there is a theoretical formulation for the *σ–ε* relationship, one can obtain a solution by direct integration of formula (1). The examples 3.1.1 and 3.1.2 show a comparison of a few different ways of a numerical solution of the governing nonlinear equation. Solutions of both problems by the regular Newton-Raphson method is compared to the solution by two simple incremental-iterative procedures with different ways to choose the step Δu for the displacement increment and to expose the above Energy-equivalent approach. The results are given in a tabular form; the first four tables are for the concrete column and the next four tables are for the steel bar:

– Tab. 1 and Tab. 5 give the numerical solutions by Newton-Raphson method.

The bolded value $\boldsymbol{\varepsilon_{form.(2)}}$ under Tab. 1 is the final strain value calculated by formula (2), for example 3.3.1 (Concrete column); the bolded value $\boldsymbol{\varepsilon_{form.(2)}}$ under the Tab. 5 is the final strain value calculated by formula (2), for example 3.3.2 (Steel bar).

– Tab. 2 and Tab. 6 give the numerical solutions obtained by using the following incremental-iterative scheme:

$$\{u^{k+1}\} = \{u^k\} + k.0{,}1.\{u_{perf.el}\}; \{\Delta u\} = k.0{,}1.\{u_{perf.el.}\}, k = 1, 2, \dots, n. \tag{12}$$

– Tab. 3 and Tab. 7 give the numerical solutions obtained by using the following incremental-iterative scheme:

$$\{u^{k+1}\} = \{u^k\} + k.0{,}1.\left\{\frac{F.L}{A.E^{k=1}}\right\} = \{u^k\} + k.0{,}1.\left\{\frac{F.L}{A.E(u_{perf.el})}\right\}, k = 1, 2, \dots, n; \tag{13}$$

$$\{\Delta u\} = k.0{,}1.\left\{\frac{F.L}{A.E(u_{perf.el})}\right\}, k = 1, 2, \dots, n.$$

For this solution, the displacement increment $\{\Delta u\} = k.0{,}1.\left\{\frac{F.L}{A.E(u_{perf.el})}\right\}$ for the $\{u\}$ is used, instead of the increment $\{\Delta u\} = k.0{,}1.\left\{\frac{F.L}{A.E(u=0)}\right\}$, since this prediction gives faster solution convergence; here $E(u = 0) = E_0$ is the modulus of elasticity (Young's modulus).

– Tab. 4 and Tab. 8 give the numerical solutions obtained by the above exposed methodology using an energy-equivalent modulus in each step.

The bolded numerical values at the first line under Tab. 2, Tab. 3 and Tab. 4 are the final values of the displacements and the strains which correspond exactly to the compressive load of -12,0 MN, calculated for example 3.3.1 (Concrete column); the bolded numerical values at the second line are the difference in % between these displacements and strains, while the bolded values at the first and the second columns of Tab. 1 – the obtained by the Newton-Raphson method.

The bolded numerical values at the first line under Tab. 6, Tab. 7 and Tab. 8 are the final values of the displacements and the strains which correspond exactly to the tensile load of 50 MN, calculated for example 3.3.2 (Steel bar); the bolded numerical values at the second line are the difference in % between these displacements and strains, while the bolded values at the first and second columns of Tab. 5 – the obtained by the Newton-Raphson method.

3.1.1. Concrete column, concrete C30/37, loaded to compression

The σ–ε relationship is set by formula (1) $\sigma(\varepsilon) = \sigma_{lim}.\tanh\left(\frac{\varepsilon}{\varepsilon_{rul}}\right)$, with σ_{lim} = 26,0 MPa, ε_{rul} = 0,00078 → E_0 = 33 333 MPa, and data for the column A = 0,5 m^2, L = 3 m, F = -12,0 MN.

Table 1. Numerical solution by Newton-Raphson method

u_i	$\varepsilon = u_i/L$	$\sigma(\varepsilon)$	$\varphi(\varepsilon) = A.\sigma(\varepsilon) - F$	u_{i+1}	F
0,000000	0,000000	0,000	12,000	-0,000720	0,000
-0,002160	-0,000720	-18,911	2,544	-0,002484	-9,456
-0,002484	-0,000828	-20,443	1,778	-0,002764	-10,222
-0,002764	-0,000921	-21,522	1,239	-0,003000	-10,761
-0,003000	-0,001000	-22,282	0,859	-0,003194	-11,141
-0,003194	-0,001065	-22,816	0,592	-0,003348	-11,408
-0,003348	-0,001116	-23,188	0,406	-0,003467	-11,594
-0,003467	-0,001156	-23,447	0,277	-0,003556	-11,723
-0,003556	-0,001185	-23,625	0,187	-0,003621	-11,813
-0,003621	-0,001207	-23,747	0,127	-0,003667	-11,873
-0,003667	-0,001222	-23,830	0,085	-0,003698	-11,915
-0,003698	-0,001233	-23,886	0,057	-0,003720	-11,943
-0,003720	-0,001240	-23,924	0,038	-0,003735	-11,962
-0,003735	-0,001245	-23,949	0,026	-0,003745	-11,974
-0,003745	-0,001248	-23,966	0,017	-0,003752	-11,983
-0,003752	-0,001251	-23,977	0,011	-0,003757	-11,989
-0,003757	-0,001252	-23,985	0,008	-0,003760	-11,992
-0,003760	-0,001253	-23,990	0,005	-0,003762	-11,995
-0,003762	-0,001254	-23,993	0,003	-0,003763	-11,997
-0,003763	-0,001254	-23,995	0,002	-0,003764	-11,998
-0,003764	**-0,001255**	-23,997	0,002	-0,003765	-11,998
-0,003765	-0,001255	-23,998	0,001	-0,003765	-11,999
-0,003765	-0,001255	-23,999	0,001	-0,003766	-11,999
-0,003766	-0,001255	-23,999	**0,000**	**-0,003766**	**-12,000**
-0,003766	-0,001255	-23,999	0,000	-0,003766	-12,000
-0,003766	-0,001255	**-24,000**	0,000	-0,003766	-12,000

$\varepsilon_{form.(2)}$ = **-0,001255**

This example is presented to illustrate the comparison between the regular Newton-Raphson method and two alternative iterative methods. In fact, such a concrete column would break down as a result of transfer tensional stresses which could be up to 20 times less than the compressive cub strength of a concrete. More realistic nonlinear behavior of concrete is illustrated in examples in Section 3.4 and in Section 3.5. The *σ–ε* curve is depicted in Fig. 7.

Table 2. Numerical solution by simplified incremental formula (12)

u_i	$\varepsilon = u_i/L$	$E(\varepsilon) = \partial\sigma(\varepsilon)/\partial\varepsilon$	$\sigma(\varepsilon) = \varepsilon.E(\varepsilon)$	$\sigma = f(\varepsilon)$	F
0,000000	0,000000	33 333	0,000	0,000	0,000
-0,002160	-0,000720	15 699	-11,303	-18,911	-9,456
-0,002376	-0,000792	13 674	-10,829	-19,967	-9,984
-0,002614	-0,000871	11 652	-10,151	-20,969	-10,484
-0,002851	-0,000950	9 858	-9,369	-21,819	-10,910
-0,003089	-0,001030	8 290	-8,535	-22,536	-11,268
-0,003326	-0,001109	6 935	-7,689	-23,138	-11,569
-0,003564	-0,001188	5 777	-6,863	-23,640	-11,820
-0,003802	-0,001267	4 795	-6,076	-24,058	-12,029

-0,003769 -0,001256
δ_u = -0,09 % δ_ε = -0,12 %

Table 3. Numerical solution by simplified incremental formula (13)

u_i	$\varepsilon = u_i/L$	$E(\varepsilon) = \partial\sigma(\varepsilon)/\partial\varepsilon$	$\sigma(\varepsilon) = \varepsilon.E(\varepsilon)$	$\sigma = f(\varepsilon)$	F
0,000000	0,000000	33 333	0,000	0,000	0,000
-0,002160	-0,000720	15 699	-11,303	-18,911	-9,456
-0,002619	-0,000873	11 612	-10,136	-20,988	-10,494
-0,003077	-0,001026	8 361	-8,576	-22,504	-11,252
-0,003536	-0,001179	5 904	-6,959	-23,585	-11,793
-0,003995	-0,001332	4 112	-5,475	-24,343	-12,172

-0,003787 -0,001262
δ_u = -0,56 % δ_ε = -0,60 %

Table 4. Numerical solution by Energy-equivalent approach

$E(\varepsilon)_{equiv}$	u_i	$\varepsilon = u_i/L$	W_{plast}	$E(\varepsilon)_{equiv}$	$\sigma(\varepsilon) = \tanh(\varepsilon/\varepsilon_{lim})$	F
33 333	-0,002160	-0,000720	0,007635	29 457	-18,911	-9,456
29 457	-0,002376	-0,000792	0,009036	28 810	-19,967	-9,984
28 810	-0,002592	-0,000864	0,010507	28 151	-20,884	-10,442
28 151	-0,002808	-0,000936	0,012040	27 486	-21,675	-10,838
27 486	-0,003024	-0,001008	0,013626	26 820	-22,353	-11,176
26 820	-0,003240	-0,001080	0,015256	26 160	-22,931	-11,466
26 160	-0,003456	-0,001152	0,016926	25 508	-23,423	-11,712
25 508	-0,003672	-0,001224	0,018628	24 867	-23,839	-11,920
24 867	-0,003888	-0,001296	0,020357	24 240	-24,191	-12,096

-0,003771 -0,001257
δ_u = -0,13 % δ_ε = -0,17 %

3.1.2. Steel bar loaded to tension

The σ–ε relationship is set again by formula (1), using the next values: σ_{lim} = 550,0 MPa, ε_{rul} = 0,002619, E_0 = 210 004 MPa, A = 0,1 m^2, L = 3 m, F = 50 MN. The σ–ε curve is depicted in Fig. 8. The more realistic nonlinear behavior of steel is illustrated in the example in Section 3.3.

Table 5. Numerical solution by Newton-Raphson method

u_i	$\varepsilon = u_i/L$	$\sigma(\varepsilon)$	$\varphi(\varepsilon) = A.\sigma(\varepsilon) - F$	u_{i+1}	F
0,000000	0,000000	0,000	-0,500	0,002381	0,000
0,007143	0,002381	396,383	-0,104	0,008169	0,396
0,008169	0,002723	427,786	-0,072	0,009040	0,428
0,009040	0,003013	449,864	-0,050	0,009761	0,450
0,009761	0,003254	465,369	-0,035	0,010342	0,465
0,010342	0,003447	476,215	-0,024	0,010794	0,476
0,010794	0,003598	483,759	-0,016	0,011136	0,484
0,011136	0,003712	488,970	-0,011	0,011386	0,489
0,011386	0,003795	492,544	-0,007	0,011566	0,493
0,011566	0,003855	494,979	-0,005	0,011691	0,495
0,011691	0,003897	496,629	-0,003	0,011778	0,497
0,011778	0,003926	497,741	-0,002	0,011838	0,498
0,011838	0,003946	498,489	-0,002	0,011878	0,498
0,011878	0,003959	498,990	-0,001	0,011905	0,499
0,011905	0,003968	499,326	-0,001	0,011924	0,499
0,011924	0,003975	499,550	**0,000**	0,011936	**0,500**
0,011936	0,003979	499,700	0,000	0,011944	0,500
0,011944	0,003981	499,800	0,000	0,011949	0,500
0,011949	0,003983	499,867	0,000	0,011953	0,500
0,011953	0,003984	499,911	0,000	0,011956	0,500
0,011956	0,003985	499,941	0,000	0,011957	0,500
0,011957	0,003986	499,960	0,000	0,011958	0,500
0,011958	0,003986	499,974	0,000	0,011959	0,500
0,011959	0,003986	499,982	0,000	0,011959	0,500
0,011959	0,003986	499,988	0,000	0,011960	0,500
0,011960	**0,003987**	499,992	0,000	**0,011960**	0,500
0,011960	0,003987	499,995	0,000	0,011960	0,500
0,011960	0,003987	499,997	0,000	0,011960	0,500
0,011960	0,003987	499,998	0,000	0,011960	0,500
0,011960	0,003987	499,998	0,000	0,011960	0,500
0,011960	0,003987	499,999	0,000	0,011960	0,500
0,011960	0,003987	499,999	0,000	0,011960	0,500
0,011960	0,003987	**500,000**	0,000	0,011960	0,500

$\varepsilon_{form.(2)}$ = **0,003987**

Table 6. Numerical solution by simplified incremental formula (12)

u_i	$\varepsilon = u_i/L$	$E(\varepsilon) = \partial\sigma(\varepsilon)/\partial\varepsilon$	$\sigma(\varepsilon) = \varepsilon.E(\varepsilon)$	$\sigma = f(\varepsilon)$	F
0,000000	0,000000	210 004	0,000	0,000	0,000
0,007143	0,002381	100 927	240,299	396,383	0,396
0,007857	0,002619	88 196	230,986	418,877	0,419
0,008643	0,002881	75 434	217,317	440,274	0,440
0,009428	0,003143	64 055	201,313	458,510	0,459
0,010214	0,003405	54 062	184,065	473,948	0,474
0,011000	0,003667	45 393	166,437	486,943	0,487
0,011786	0,003929	37 949	149,083	497,832	0,498
0,012571	0,004190	31 611	132,464	506,918	0,507

0,011973 0,003991
δ_u = -0,11 % δ_ε = -0,11 %

Table 7. Numerical solution by simplified incremental formula (13)

u_i	$\varepsilon = u_i/L$	$E(\varepsilon) = \partial\sigma(\varepsilon)/\partial\varepsilon$	$\sigma(\varepsilon) = \varepsilon.E(\varepsilon)$	$\sigma = f(\varepsilon)$	F
0,000000	0,000000	210 004	0,000	0,000	0,000
0,007143	0,002381	100 927	240,299	396,383	0,396
0,008629	0,002876	75 645	217,580	439,928	0,440
0,010115	0,003372	55 246	186,273	472,145	0,472
0,011601	0,003867	39 590	153,098	495,452	0,495
0,013088	0,004363	27 987	122,094	512,041	0,512

0,012009 0,004003
δ_u = -0,41 % δ_ε = -0,41 %

Table 8. Numerical solution by Energy-equivalent approach

$E(\varepsilon)_{equiv}$	u_i	$\varepsilon = u_i/L$	W_{plast}	$E(\varepsilon)_{equiv}$	$\sigma(\varepsilon) = \tanh(\varepsilon/\varepsilon_{lim})$	F
210 004	0,007143	0,002381	0,527727	186 189	396,383	0,396
186 189	0,007857	0,002619	0,624840	182 191	418,877	0,419
182 191	0,008571	0,002857	0,726957	178 111	438,465	0,438
178 111	0,009286	0,003095	0,833419	173 989	455,413	0,455
173 989	0,010000	0,003333	0,943629	169 859	469,994	0,470
169 859	0,010714	0,003571	1,057056	165 752	482,479	0,482
165 752	0,011428	0,003809	1,173231	161 692	493,123	0,493
161 692	0,012143	0,004048	1,291745	157 697	502,168	0,502

0,011971 0,003990
δ_u = -0,10 % δ_ε = -0,13 %

3.2. FEM examples solved by Energy-equivalent approach

The following examples, presented in Sections 3.3.1, 3.3.2 and 3.3.3, are solved with a FEM program, compiled by the author on Excel Visual Basic ([19]), using the analytical formulas for stresses. This imposes some computational restrictions for the maximum strain in the concrete tensile zone (Sections 3.4, 3.5). Plane triangular isoparametric finite elements are used (according to [20, 21]), as shown in Fig. 9. The depicted finite element scheme in Fig. 9 is principally correct, but not fully precise. The finite element mesh is presented only as a picture and depicts twice fewer elements in both length and height.

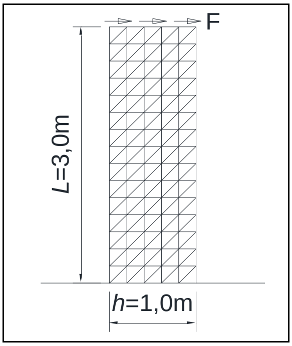

Figure 9. Finite element scheme for the calculations

Since there is practically no linear part in stress-strain curves of hyperbolic type used in the examples (in principle, the Poisson's ratio is mostly applied within the elastic region of the stress-strain relationship), and the corresponding curvilinear dependence completely defines the stress-strain state for the particular case, and also in order to avoid obtaining a non-symmetric stiffness matrix and for simplification of the calculation, for simplification a Poisson's ratio $\nu = 0$ is adopted. In such a way the problems become physically equivalent to the Euler–Bernoulli beam theory and the pure bar tension/compression, which correspond to the classical Hook's Law ("ut tensio, sic vis,"), i.e., "perfectly" compressible solid, without any transverse deformations. In this case, the Plane Stress and Plane Strain formulations are completely identical. In the three examples, the same geometric model was used – a cantilever beam with fixed lower end and uniform distributed load at free end, perpendicular to the axis of the structure. The model has 61 nodes and 60 finite elements along the length of the beam and 21 nodes and 20 elements along the height. The beam has a rectangular cross section. The geometrical dimensions of the model and the type of load are shown in Fig. 9.

3.2.1. Cantilever stainless steel beam subjected to bending and shearing

The σ–ε relationship is set by formula (1), using values σ_{lim} = 550 MPa and ε_{rul} = 0,002619; t = 0,10 m, F = 6,0 MN. The normal stresses and the tangential stresses along the height of the cross section at the fixed end are shown in Fig. 10 and Fig. 11. The continuous line depicts the results obtained after 15 iterations, the dotted line – after 5 iterations and the dashed line – after 3 iterations. The normal stresses along the height of the cross sections at the middle of the beam in length and at the loaded end are shown in Fig. 12 and in Fig. 13, respectively. They are obtained after 15 iterations. The transversal displacements tend to final value and the solution is convergent (Fig. 16). The maximum transversal displacement at a node of the loaded end after the 3-rd iteration is -0,041 m, after the 5-th iteration is -0,0425 m and after the 15-th iteration is -0,043 m.

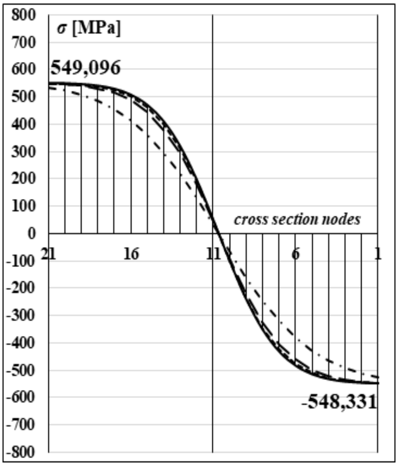

Figure 10. σ_{max} **vs** h **for loading 6,0 MN**

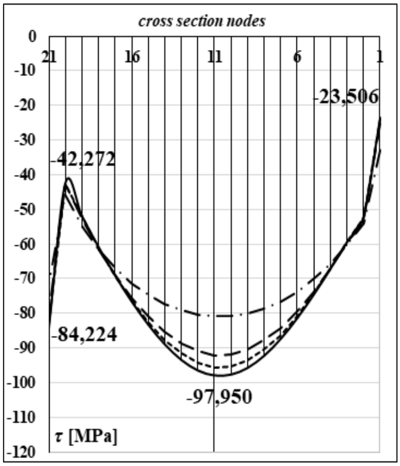

Figure 11. τ_{max} **vs** h **for loading 6,0 MN**

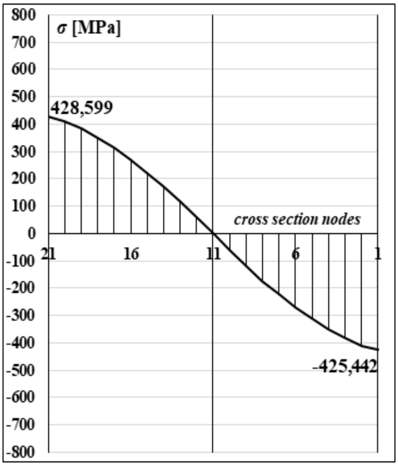

Figure 12. $\sigma_{1/21}$ **vs** h **for loading 6,0 MN**

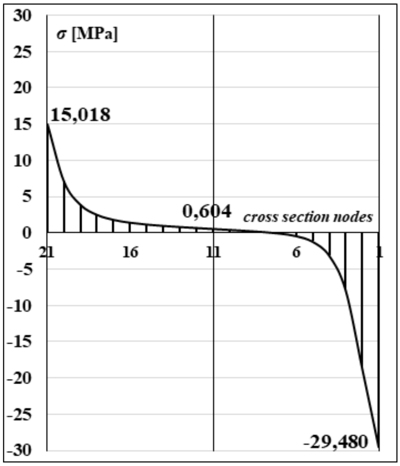

Figure 13. σ_{l} **vs** h **for loading 6,0 MN**

Load F = 6,0 MN is the maximum value which this construction can withstand without destroying. If we set greater load than 6 MN, the beam continues to deform, and the mathematical solution does not converge. Dividing the external load into small steps, we can obtain the maximum loading value. In loading case F = 10,0 MN displacements increase permanently after each iteration and there is no solution convergence – the beam will fail due to applied force. This is illustrated in Fig. 17. The diagrams of the maximum normal and tangential stresses at the fixed end of the beam after the 25-th iteration for loading case F = 10,0 MN are shown in Fig. 14 and in Fig. 15, respectively. The maximum transversal displacements at a node of the loaded end for loading case F = 6,0 MN are shown in Fig. 16 and for loading case F = 10,0 MN in Fig. 17.

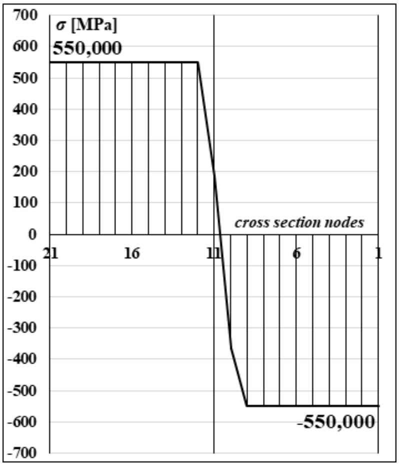

Figure 14. σ_{max} **vs** h **for loading 10,0 MN**

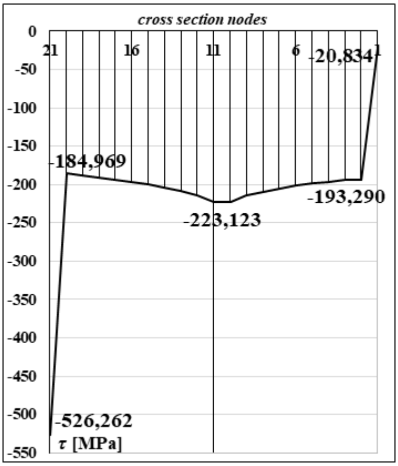

Figure 15. τ_{max} **vs** h **for loading 10,0 MN**

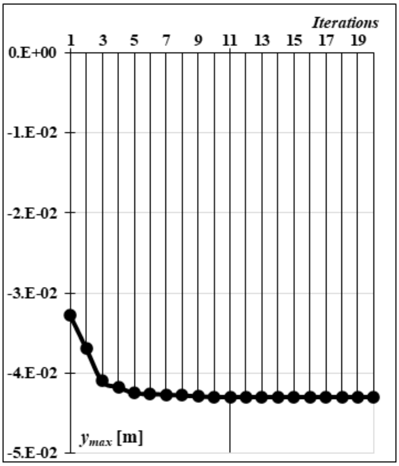

Figure 16. Displacements for loading 6,0 MN

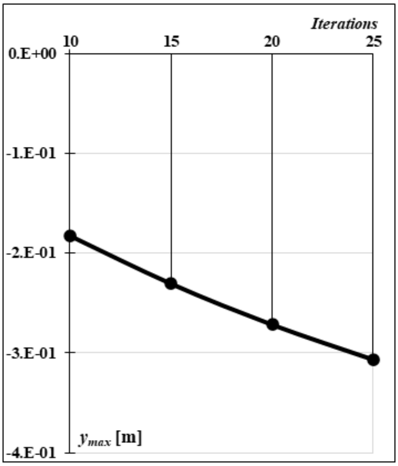

Figure 17. Displacements for loading 10,0 MN

Maximum displacements at a node of the loaded end vs numbers of the iterations for the loading cases 6,0 MN and 10,0 MN

3.2.2. Cantilever column, concrete C30/37, subjected to bending and shearing

Two results are presented for two loading cases that lead to two fundamentally different failure cases. The σ–ε relationship for this example is set by the following formula:

$$\sigma(\varepsilon) = \sigma_{lim} \cdot \frac{e^{\frac{\varepsilon - 0{,}0001}{\varepsilon_{rul,1}}} - 0{,}84545}{e^{\frac{\varepsilon - 0{,}0001}{\varepsilon_{rul,2}}} + 1}, \tag{14}$$

where: σ_{lim} =24,081 MPa, $\varepsilon_{rul,1}$ =0,00059569, $\varepsilon_{rul,2}$ = 0,00003; t = 0,25 m, F = 0,03 MN. The graphic of the σ–ε curve is depicted in Fig. 18 and the function $E(\varepsilon)$ for this stress-strain relationship is depicted in Fig. 19.

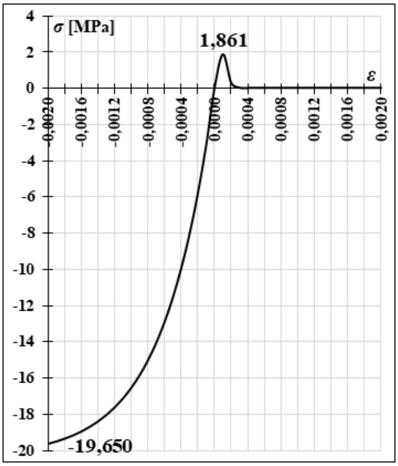

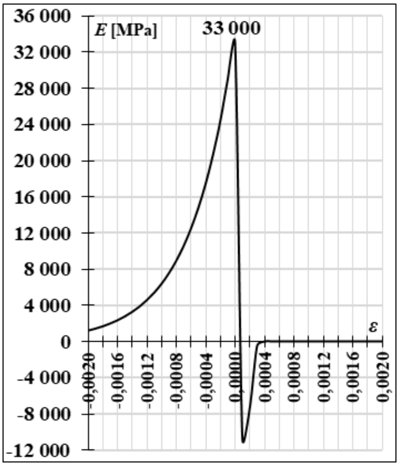

Figure 18. $\sigma(\varepsilon)$ **by formula (14)**

Figure 19. $E(\varepsilon)$ **by formula (14)**

Formula (14) is a result of a more general formula using the corresponding values for σ_{lim}, $\varepsilon_{rul,1}$ and $\varepsilon_{rul,2}$. The results for the stresses and the displacements after the 5-th iteration and the 20-th iteration are equal. The normal stresses and the tangential stresses diagrams along the height of the column cross section at the fixed end are depicted in Fig. 20 and Fig. 21, respectively. The normal stresses along the height of the cross sections in the middle of the beam in length and at the loaded end are shown in Fig. 22 and in Fig. 23, respectively. The maximum transversal displacement at a node of the loaded end is -0,0004 m for all iterations. The convergence of the solution breaks at $\varepsilon_{\max\ tens} \approx 0{,}00009$ when $\sigma = \sigma_{\max\ tens} \approx 1{,}935$ MPa and $E(\varepsilon_{\max\ tens}) = 0$ MPa.

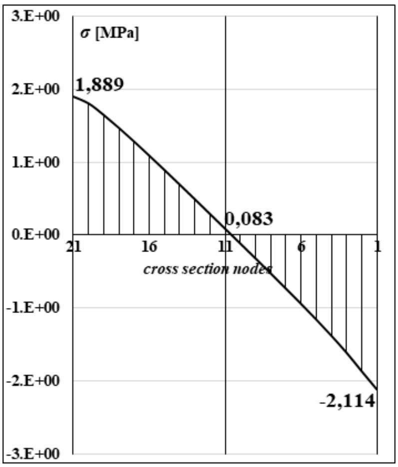

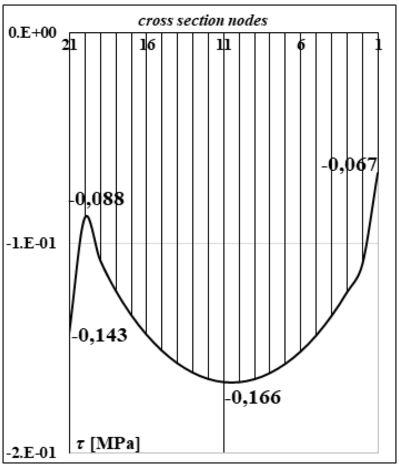

Figure 20. $\sigma_{\max}$ **vs** h **for loading 0,03 MN**

Figure 21. $\tau_{\max}$ **vs** h **for loading 0,03 MN**

The σ–ε relationship for the next results in this example is also set by formula (14) with the same values for the geometric and physical properties of the beam (Fig. 9) but for load F=0,10 MN. Since the load-bearing capacity of the concrete in the tensile zone is lower than the stresses caused by the applied load, the structure will fail. At each successive iteration the displacements, respectively the strains, continue to increase without tending to any finite value.

The solution fails at the 5-th iteration – one or more terms on the main diagonal of the stiffness matrix become 0. This can be considered the load at which the first crack occurs in this area of a structure of brittle material (one or several finite elements of the model get modules $E_{ij} = 0$).

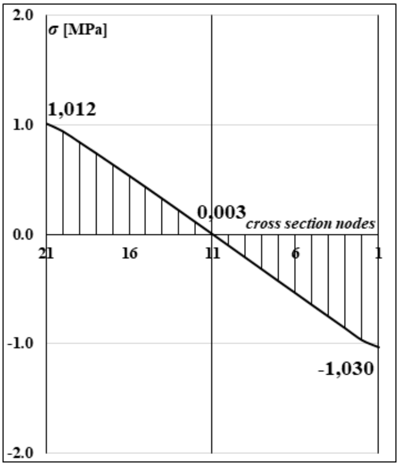

Figure 22. $\sigma_{1/21}$ **vs** h **for loading 0,03 MN**

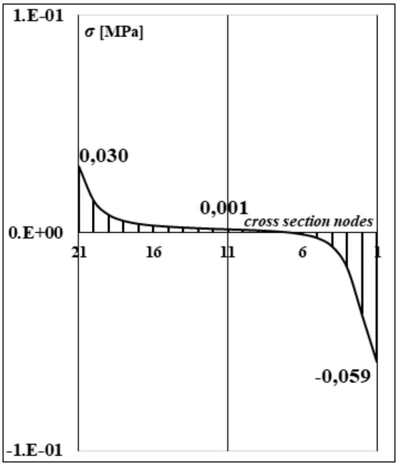

Figure 23. σ_1 **vs** h **for loading 0,03 MN**

If we divide the load into small equal steps, e.g., F = 0,01 MN, we can determine the maximum load this construction can withstand without being destroyed. In such a way the used in the example a load of F = 0,03 MN (or slightly larger) is obtained. The maximum normal and tangential stresses at the fixed end of the column after the 4-th iteration are shown in Fig. 24 and Fig. 25, respectively. If we set, e.g., 1,0 MPa as a minimum value for the nonlinear modulus at each finite element, we avoid receiving 0 in the stiffness matrix main diagonal and we can continue the calculation to the very end. The maximum normal and tangential stresses after the 20-th iteration are shown in Fig. 26 and Fig. 27, respectively. The maximum transversal displacements at a node of the loaded end of the column are shown in Fig. 28. After the 4-th iteration the displacements do not break and tend to some final but enormous value because a minimum value for the nonlinear modulus at each finite element in this case is set to 1,0 MPa.

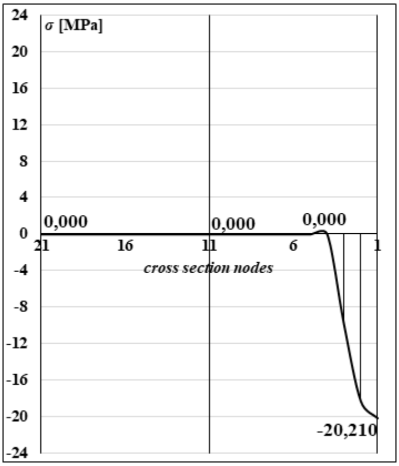

Figure 24. σ_{max} **vs** h **after 4-th iteration**

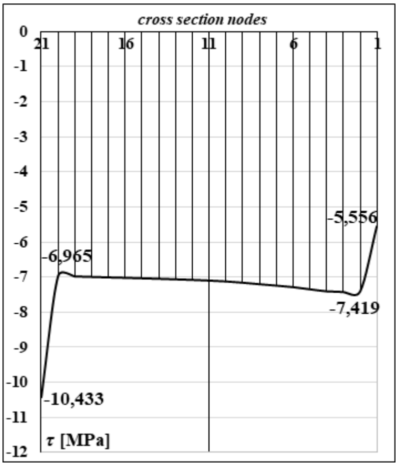

Figure 25. τ_{max} **vs** h **after 4-th iteration**

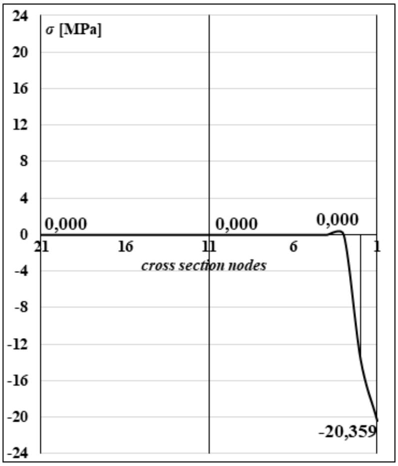

Figure 26. σ_{max} vs *h* after 20-th iteration

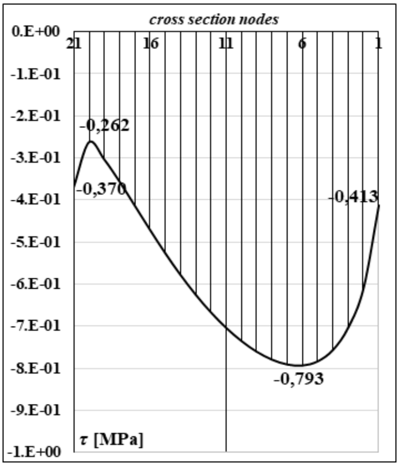

Figure 27. τ_{max} vs *h* after 20-th iteration

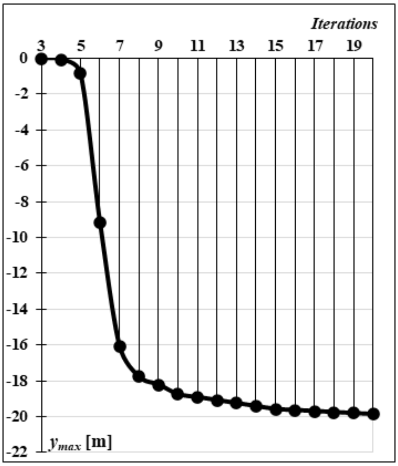

Figure 28. Max displacements vs numbers of the iterations for loading case *F* = 0,10 MPa

3.2.3. Cantilever reinforcement concrete column, concrete C30/37, stainless steel B500B, subjected to bending and shearing

For this example, the σ–ε relationship is set also by formula (14) (Fig. 18). The geometric scheme of the column and the type of load are the same as in the previous example (Fig. 9), but the load is *F* = 0,40 MN. The basic difference in this example compared to the previous is that 60 classical bar finite elements have been added in the FE model to the second column of nodes from left to right to simulate a reinforcement. In this way one reinforcement B500B stainless-steel bar Ø8 with area of 0,503 cm^2 is added at the beam tensile zone. This may not be the best way to simulate a reinforcement, but it is good enough from a practical point of view, to give us an idea of the effect of adding steel bars to a concrete cross section. The reinforcement axis is set on 5 cm from the lateral edge and the clear concrete cover is 4,6 cm. A nonlinear σ–ε relationship set by formula (1) with σ_{lim} = 550,0 MPa and ε_{rul} = 0,002619 is assumed for the added 60 B500B stainless steel beam elements in this example. The normal stresses and the tangential stresses along the height of the cross section at the fixed end are shown in Fig. 29 and Fig. 30, respectively. The normal stresses along the height of the cross section in the middle of the beam in length and at the loaded end are shown in Fig. 31 and in Fig. 32, respectively. These results are obtained after only 5 iterations. The maximum normal stress in the stainless-steel bar Ø8 at the node of the fixed end is σ = 144,917 MPa. The maximum transversal displacement at a node of the loaded end (in the negative direction of the relevant axis) is -0,0025 m. The difference in the results for the stresses obtained after the 20-th iteration by dividing the load into 10 equal steps of F_i = 0,04 MN each is -0,005 MPa for the maximum normal stress ($\sigma_{\max}$ = -14,555 MPa, compression) and -0,072 MPa for the maximum tangential stress ($\tau_{\max}$ = -2,435 MPa); the maximum normal stress in the stainless-steel bar Ø8 is $\sigma_{\max}$ =1 71,658 MPa (tension).

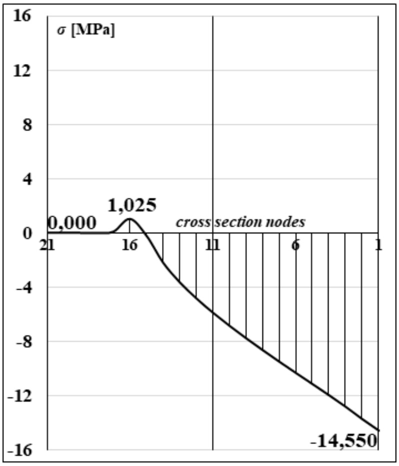

Figure 29. $\sigma_{\max}$ vs h for loading 0,40 MN

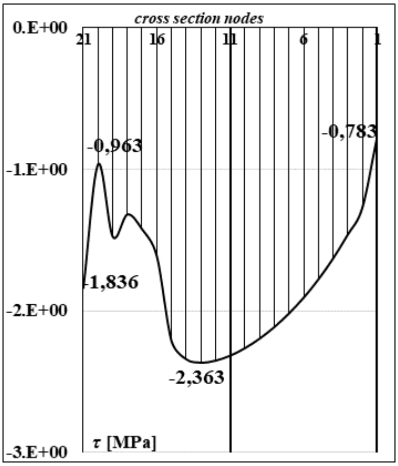

Figure 30. $\tau_{\max}$ vs h for loading 0,40 MN

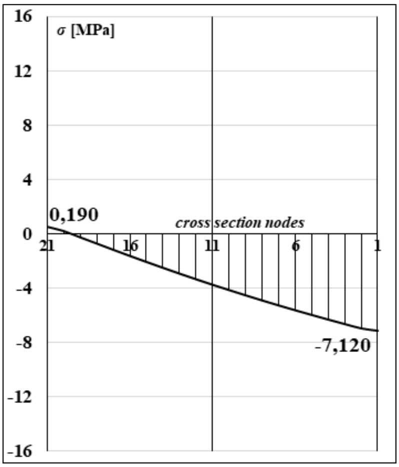

Figure 31. $\sigma_{1/21}$ vs h for loading 0,40 MN

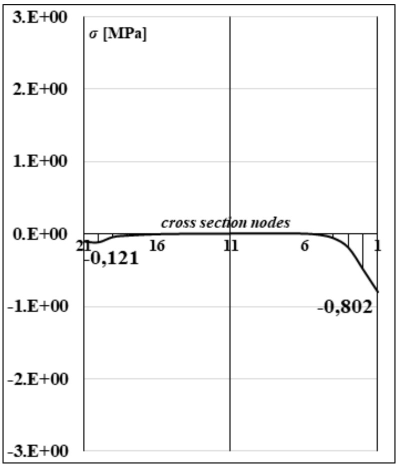

Figure 32. σ_1 vs h for loading 0,40 MN

The σ–ε relationship for the next results in this example is set by formula (14) with the same values for the geometric and physical properties of the beam but for load F = 0,80 MN and F = 2,0 MN. These cases are analogical to the corresponding loading cases of the previous example – the column has no sufficient load-bearing capacity to support applied external load.

The computation fails for the same reasons – one or few terms of the stiffness matrix main diagonal become 0. If we set, e.g., 1,0 MPa as a minimum value for the nonlinear modulus at each finite element, as in the previous example, we avoid receiving 0 in the stiffness matrix main diagonal and we can continue the calculation to the very end. For load F = 0,80 MN the solution fails at the 11-th iteration. The normal stresses along the height of the cross section at the fixed end after the 10-th iteration, but without setting E_{min} = 1,0 MPa, and after the 25-th iteration are shown in Fig. 33 and in Fig. 34, respectively. The maximum normal stress in the stainless-steel bar ∅8 at the node of the fixed end is σ = 246,991 MPa after the 10-th iteration (in this case E_{min} = 0), σ = 398,273 MPa after the 25-th iteration and σ = 500,139 MPa after the 30-th iteration (E_{min} =1,0 MPa).

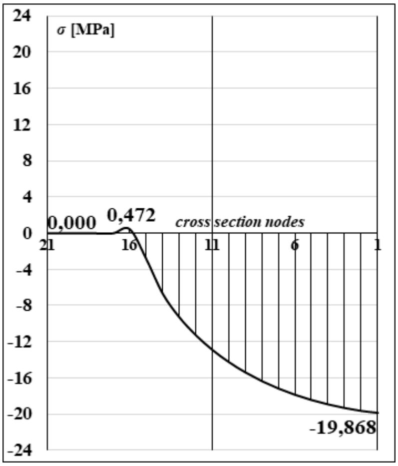

Figure 33. σ_{max} vs *h* at 10-th iteration

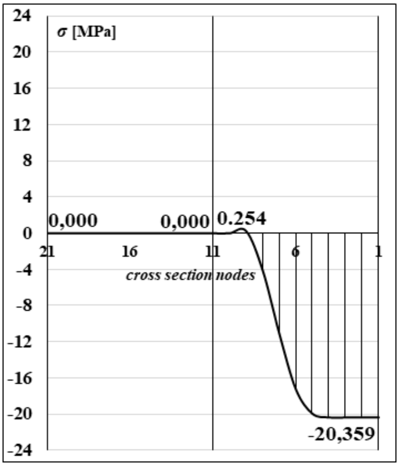

Figure 34. σ_{max} vs *h* at 25-th iteration

Maximum normal stresses in the concrete at the fixed end for loading case *F* = 0,80 MN

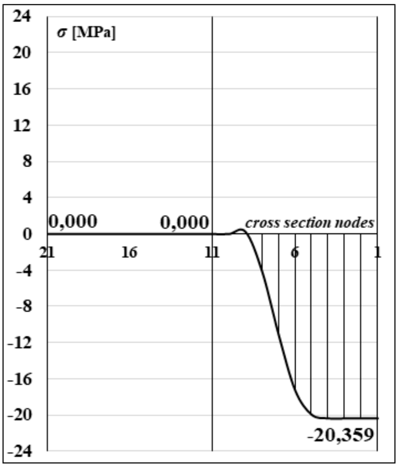

Figure 35. σ_{max} vs *h* at 3-th iteration

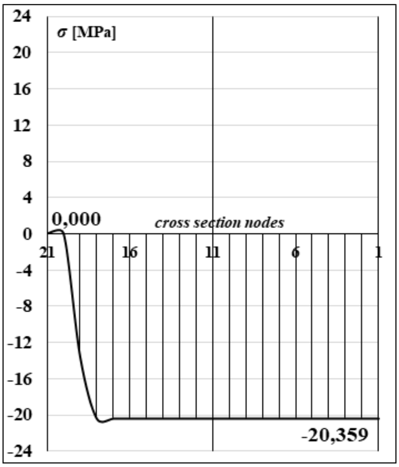

Figure 36. σ_{max} vs *h* at 10-th iteration

Maximum normal stresses in the concrete at the fixed end for loading case *F* = 2,0 MN

For load F = 2,0 MN the solution fails at the 4-th iteration. The diagrams of the maximum normal stresses in the concrete at the fixed end after the 3-th iteration, without setting E_{min} = 1,0 MPa, and the 10-th iteration are shown in Fig. 35 and in Fig. 36, respectively. The maximum normal stress in the stainless-steel bar Ø8 at the node of the fixed end after the 3-th iteration is σ = 461,845 MPa and σ = 550,0 MPa after the 10-th iteration, but in the next three nodes by length.

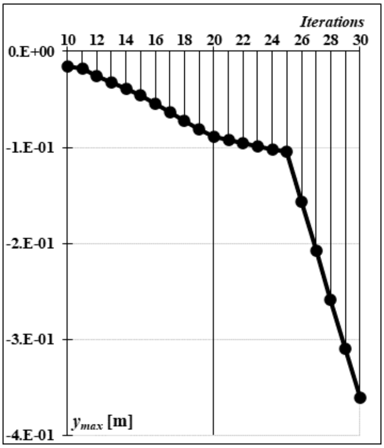

Figure 37. Maximum displacements vs numbers of the iterations for loading cases *F* = 0,80 MN

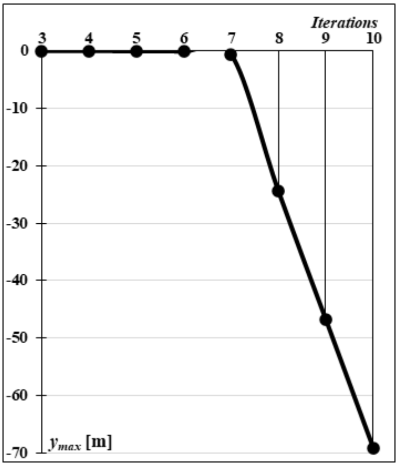

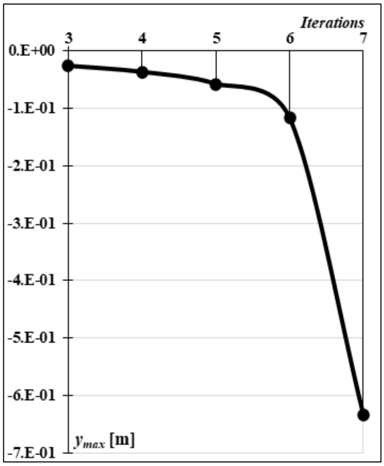

Figure 38. Displacements to 10-th iteration   **Figure 39. Displacements to 7-th iteration**

Maximum displacements vs numbers of the iterations for loading cases *F* = 2,0 MN

The maximum displacements at a node of the loaded end of the column for loading case F = 0,80 MN are shown in Fig. 37, the first figure in the row. The maximum displacements at a node of the loaded end for loading case F = 2,0 MN are shown in Fig. 38. The initial part of Fig. 38, up to the 7-th iteration at a larger scale, is depicted in Fig. 39. Since the load in this case is too large, the displacements do not tend to some final value, as in the previous example, but become unrealistically big after only a few iterations. These results are obtained after a minimum value for the nonlinear modulus at each finite element of 1,0 MPa is set.

4. Conclusions and future work

The presented original method is powerful instrument for solving the system of nonlinear FEM equations obtained for solids with material nonlinearity defined by many various types of stress–strain relationship. Using the Energy-equivalent approach in the standard FEM leads to a very fast convergence of the solution compared to the Newton-Raphson method and other classical methods, since it is not necessary to divide the load into small-time steps. If this is still done, minor increase in the calculation accuracy when integrating the strain energy can be obtained, but at the expense of a significant increase in computational work. Dividing the external load into small steps and applying it in successive increments is necessary only to determine the load-bearing capacity of the investigated structural element with material nonlinearity or of an entire structure with material nonlinearity in some critical point. For a load that the individual structural element or the whole structure can withstand without destruction in certain area, the solution is completely convergent, and the displacements and stresses tend to some finite values. This is illustrated in the examples of Sections 3.3, 3.4 and 3.5 – one load within the load-bearing capacity of the steel beam, the concrete column and reinforced concrete column, and another larger load that causes the structures to collapse.

The Energy-equivalent approach and the advantages of the proposed first prediction for displacements allows very easily to find a solution for various special cases and peculiarity of the σ–ε curves, where many other methods fail or become extremely inefficient. This enables the proposed Energy-equivalent approach to use any type of True Stress–True Strain relationship without restrictions, regardless of their complexity. Also, the presented methodology for solving nonlinear equations could be very easily incorporated into any commercial or other FEM program for solving problems of material nonlinearity in the field of solid mechanics. The method can be applied both to 2D and 3D problems in the Finite element method. This would enable relatively more easily to refine the actual nonlinear behavior both of single structural elements and of entire large structures. It would be particularly useful to do this not only for a static problem, but above all for dynamic and especially for seismic impact cases when the seismic action applies as equivalent static forces. The presented methodology can be a very fruitful procedure in inelastic seismic pseudo static analysis, especially in reinforcement concrete structures assessment. The latter is a very interesting and important issue in seismic design as well as in general, e.g. [22 – 24], etc. For example, the application of this methodology into Pushover analysis to determine the capacity curve would make it possible to estimate the "seismic" Behavior factor in each different case relatively easily and with a high degree of reliability, and hence the actual nonlinear behavior and seismic resistance of the constructions will be evaluated more accurately. Although the methodology is presented only for the static case, it can be easily implemented to solve the seismic impact applied by an accelerogram. It is very convenient to apply in step-by-step procedures in the case of incremental formulation for dynamic nonlinear analysis where the load varies linearly in each interval Δt; this is the typical case when the load is applied by accelerograms or seismograms.

LITERATURE

1. *Varbanov, Hr. et al.* Prilozhna teoria na elastichnostta i plastichnostta. Tehnika, Sofia, 1992, ISBN 954-03-0043-8.

2. *Baltov, Ang., Popova, M*. Mehanika na materialite. Prof. Marin Drinov, Sofia, 2009, ISBN 978-954-322-278-8.

3. *Carreira, D. J., Chu, K.-H.* Stress-Strain Relationship for Plain Concrete in Compression. ACI Journal, Title no. 83-2, November-December 1985, pp.797-804.

4. *Carreira DJ, Chu K.-H.* Stress-strain relationship for reinforced concrete in tension. ACI Journal, Title no. 83-3, January-February 1986, pp.21-28.

5. *Benyahi, K. et al.* Reliability assessment of the behavior of reinforced and/or prestressed concrete beams sections in shear failure. Frattura ed Integrità Strutturale, Published by Italian Group of Fracture, 15(57), July 2021,195-222, Online ISSN: 1971-8993.

6. *Bathe, K. J.* Finite Element Procedures, Watertown, MA. Printed in the United States of America. 2nd edition: fourth printing 2016. ISBN 978-0-9790049-5-7.

7. *Bathe, K. J., Cimento, A. P.* Some practical procedures for the solution of nonlinear finite element equations. Computer Methods in Applied Mechanics and Engineering, Volume 22, Issue 1, 1980, Pages 59-85, ISSN 0045-7825.

8. *Kristensena, P. K., Martínez-Pañedab, E.* Phase field fracture modelling using quasi-Newton methods and a new adaptive step scheme. Theoretical and Applied Fracture Mechanics 107:102446, June 2020, Published by Elsevier, Print ISSN: 0167-8442.

9. *Gerasimov, T., De Lorenzis, L.* A line search assisted monolithic approach for phase-field computing of brittle fracture. Computer Methods in Applied Mechanics and Engineering 312, December 2015, Published by Elsevier, Print ISSN: 0045-7825.

10. *Lampron, O. et al.* An efficient and robust monolithic approach to phase-field quasi-static brittle fracture using a modified Newton method. Computer Methods in Applied Mechanics and Engineering, Volume 386, 2021, 114091, ISSN 0045-7825.

11. *Wambacq, J. et al.* Interior-point methods for the phase-field approach to brittle and ductile fracture. Computer Methods in Applied Mechanics and Engineering, Volume 375, 2021,113612, ISSN 0045-7825.

12. *Kim, D. et al.* Generalized finite element method with global-local enrichments for nonlinear fracture analysis. Mechanics of Solids in Brazil, 2009, Brazilian Society of Mechanical Sciences and Engineering, ISBN 978-85-85769-43-7.

13. *Ben-Shmuel, Y., Altus, E.* Modeling plasticity by non-continuous deformation, IV International Conference on Particle-based Methods – Fundamentals and Applications, Barcelona, Spain, September 2015.

14. *Monteiro, A. B. et al.* A computational framework for G/XFEM material nonlinear analysis. Advances in Engineering Software 114:380-393, August 2017, Published by Elsevier, Print ISSN: 0965-9978.

15. *Roylance D. et al.* Mechanics of materials: A materials science perspective. Proceedings of the Institution of Mechanical Engineers, Part L, Journal of Materials Design and Applications 215(3):141-145, July 2001, Published by SAGE Publications, Print ISSN: 1464-4207.

16. *Varbanov, Hr.* Teoria na elastichnostta. Tehnika, Sofia, 1962.

17. *Southwell, R. V.* Castigliano's Principle of Minimum Strain-Energy. Proceedings of the Royal Society of London. Series A – Mathematical and Physical Sciences, Volume 154, Issue 881, Mar. 1936.

18. *Varbanov, Hr.* Ustoychivost i dinamika na elastichnite sistemi. Tehnika, Sofia, 1989.

19. *Ivanova, St., Drakaliev, P.* Programirane na VBA v sredata na MS Excel. Sektor "Izdatelska deynost" pri UASG, Izdatel (kod 724) – Universitet po arhitektura, stroitelstvo i geodezia. Sofia, 2016, ISBN 978-954-724-098-8.

20. *Karamanski, T. et al.* Stroitelna mehanika. Tehnika, Sofia, 1988.

21. *Pavlova, Yu., Bankov, B.* Izchislyavane na stroitelni konstruktsii po metoda na kraynite elementi. Tehnika, Sofia, 1989.

22. *Hasan, R., Xu, L., Grierson, D. E.* Push-over analysis for performance-based seismic design. Computers & Structures, Volume 80, Issue 31, 2002, Pages 2483-2493, ISSN 0045-7949.

23. *Sonwane, D. P., Ladhane, K. B.* Seismic Performance based Design of Reinforced Concrete Buildings using Nonlinear Pushover Analysis. International Journal of Engineering Research & Technology (IJERT), Vol. 4, Issue 06, June-2015, ISSN: 2278-0181.

24. *Shehu, R.* Implementation of Pushover Analysis for Seismic Assessment of Masonry Towers: Issues and Practical Recommendations. Buildings11(2):71, February 2021, Published by MDPI AG, Online ISSN: 2075-5309.

ЕНЕРГИЙНО ЕКВИВАЛЕНТЕН МЕТОД ЗА РЕШАВАНЕ НА НЕЛИНЕЙНИ УРАВНЕНИЯ ПО МЕТОДА НА КРАЙНИТЕ ЕЛЕМЕНТИ С ИЗПОЛЗВАНЕ НА ОБОБЩЕНА ХИПЕРБОЛИЧНА ЗАВИСИМОСТ НАПРЕЖЕНИЕ-ДЕФОРМАЦИЯ

А. Александров[1]

Ключови думи: *нелинейност на материала, зависимост напрежение-деформация, хиперболични функции, малки деформации, енергия на деформацията, нелинеен анализ на крайни елементи, итеративно решение*

РЕЗЮМЕ

Представен е прост, стабилен и мощен оригинален изчислителен метод за решаване на квази-статичната задача, при който поведението на твърди тела с материална нелинейност се моделира чрез поведението на енергийно еквивалентно по отношение на енергията на деформация псевдо-перфектно еластично твърдо тяло. Този метод не се проваля за криви напрежение-деформация, имащи инфлексни точки или други особености, и математическата сходимост на решението се нарушава само когато

[1] Александър Александров, инж., ЕНЕРГОЕКСПЕРТ АД, ул. „Коста Лулчев“ № 20, 1113 София, e-mail: alexander.alexandrov.63@gmail.com

твърдите тела се разрушат физически. Убедително е показано, че подходяща класическа итеративна процедура може да бъде по-проста, по-ефективна и няколко пъти по-бърза в сравнение с обикновения, модифицирания метод на Нютон-Рафсон или други често използвани числени методи и използването на преместванията в идеалното еластично твърдо тяло като началната стойност за решаване на нелинейните уравнения има значителни предимства и е по-добра прогноза за първата итерация за преместванията в сравнение с обикновено използваната прогноза $\{d^0\}=\{0\}$.